IMPEDANCE STUDY OF A NEW SEPTUM CHAMBER OF SPEAR3*

K. Tian†, J. Langton, J. J. Sebek
SLAC National Accelerator Laboratory,Menlo Park, CA, USA

Abstract

A new in-vacuum Lambertson septum magnet has been designed for the storage ring as a part of the accelerator improvement plan for operating a lower emittance lattice in SPEAR3. Therefore it is necessary to analyze the impedance effects on the beam from the new septum chamber. Due to the complex design at the downstream transition of the septum chamber, the longitudinal impedance is of particular concern. In this paper, we will present numerical simulation results for this particular component as well as the general analysis for the impedance effects of the whole chamber.

INTRODUCTION

SPEAR3 is a 3 GeV, 500 mA, third generation light source, operating with $\epsilon_x = 10$ nm lattice. Recent developments in the SPEAR3 lattice enable the storage ring for lower emittance opeartion with $\epsilon_x < 7$ nm[**Huang17**]. In the current injection line from the booster to SPEAR3, a Lambertson-type septum magnet bends the injected beam into the storage ring plane while the stored beam passes through undeflected and captures the injected beam. The new lower emittance lattice has a smaller dynamic aperture than the current operating lattice; therefore it requires the distance between the kicked stored beam and the injected beam must be reduced to about . However, the total wall thickness for the current septum magnet is 6.5 mm. Meeting all of the challenging specifications, a new septum magnet has been designed with the wall thickness of 2.5 mm [**Joha18**]. As shown in Fig. 1, the new septum is about 1.4 meters long from flange to flange and has complex structures to allow the capture of the injected beam by the stored beam.

Before the installation of of such sophisticated vacuum components, impedance effects must first be examined. We need to evaluate the consequences of the impedance both to the beam stability and the local heating of the septum chamber. Some of these evaluations can be carried out analytically, while others require numerical simulations.

ANALYTICAL ANALYSIS

Many characteristics of the impedance of a vacuum chamber can be analyzed analytically. Such analysis guides the mechanical design of the chamber. Some design parameters concern minimizing discontinuities that create short range wakefields. Others guide the design and placement of spring fingers between sections and treatment of the chamber metal

* Work supported by US Department of Energy Contract DE-AC03-76SF00515. This research used resources of the National Energy Research Scientific Computing Center (NERSC), a U.S. Department of Energy Office of Science User Facility operated under Contract No. DE-AC02-05CH11231.

† email address:ktian@slac.stanford.edu

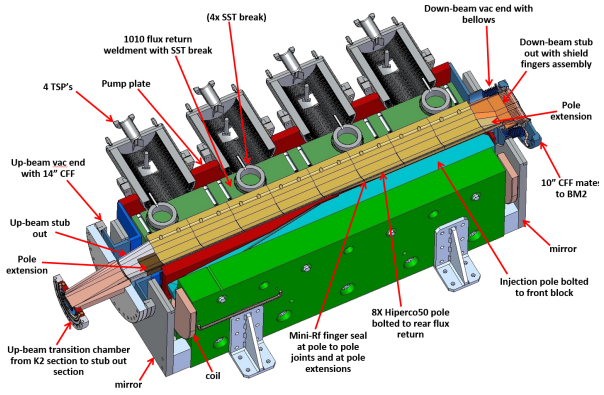

Figure 1: Section views of the new SPEAR3 injection septum magnet/chamber.

to minimize both impedance and heating. Finally one ensures that the design does not trap any radiofrequency (RF) modes that could induce inter-bunch instabilities.

Transitions

At a transition, the stored electron beam loses energy for two reasons. One is the change in the cross-section of the chamber; a larger cross-section requires the beam to generate more electromagnetic (EM) fields to fill that area. This loss is not important in a ring, as the beam recovers this energy when the cross-section returns to its original value. The more serious, and controllable, effect is due to the radiative diffraction of the fields as they encounter a transition. Analytical and numerical studies [**heifKheifRMP91**] have shown this effect is characterized by

$$\eta = \frac{l}{b-a}\frac{\sigma_B}{b-a} = \frac{l\sigma_B}{(b-a)^2}$$

where b and a are the outer and inner diameters of the taper, l is its length, and σ_B is the beam bunch length. Once $\eta > 1$ the impedance of the transition is on the asymptote to its minimum value. Our values of η are 20.2 and 6.1 for the incoming and outgoing transitions, respectively.

Image Current Distribution

We need to provide a smooth, continuous path for the beam image current flowing on the chamber walls. We use conducting fingers to create this path. We need to ensure that the fingers are densely populated where the current density is highest.

The image current distribution in a chamber is determined by the two-dimensional electric field distribution created by the bunch charge. In a parallel plate vacuum chamber, the current is strongly localized directly above and below the beam; 98% of the current is centered around the beam,

within a distance equal to three times the height of the chamber. It is mechanically most difficult to place the fingers near the vertex of the septum chamber near the injected beam. However the surface charges in such a vertex go as $\sigma_E \approx \rho^{(\pi/\beta)-1}$[**jackson99**, **smythe68**], where ρ is the radial distance from the vertex and β is its opening angle. For our septum, $\beta = \pi/3$; the charge decreases quadratically, as ρ^2, near the wall and the requirements on the placement of the fingers at the vertex can be relaxed as seen in Fig. 2.

One can guarantee only a point contact on each RF finger. Therefore better current conduction is guaranteed with many small fingers rather than a few large fingers. The fingers are mounted in recesses. The radial depths of those recesses are limited to ensure that any $\lambda/4$ resonances generated by those depths are well above the bunch cutoff frequency of 9 GHz. Our maximum allowable depth of 2.5 mm places any resonances above 30 GHz.

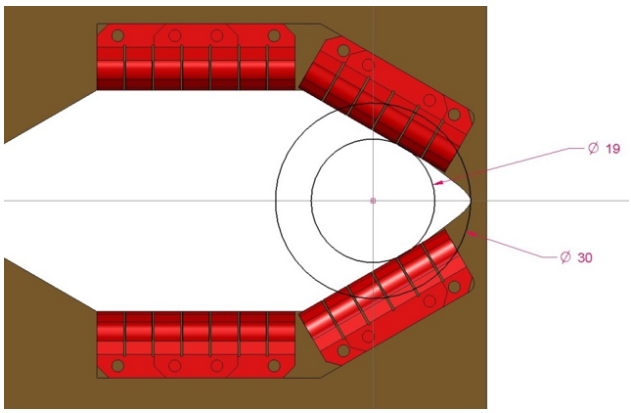

Figure 2: Location of conducting fingers at chamber flanges.

Resistive Wall Impedance

The transverse resistive wall impedance for a chamber goes as $Z_\perp \sim 1/(b^3\sigma)$, where b is the radius of the chamber and σ is the electrical conductivity of the wall. We minimize $Z_\perp$ by copper plating the wall to $> 70\,\mu$m, making the wall appear to be copper for all frequencies of interest (> 1 MHz). The heating due to the resistive wall impedance in the septum is about 1.3 W/m.

Vacuum Pumping Ports

We need sufficient vacuum conductance in the chamber to achieve our required vacuum performance. An ante-chamber was designed on the outboard side of the septum and holes were drilled in the septum wall to connect to the ante-chamber. Three rules were followed to minimize the impact of these holes on the chamber impedance. First, the holes were drilled in a wall far from the location of the beam, where the beam-generated fields are very small. Second, the diameters of the holes are small, making them above cutoff for any fields that could interact with the beam spectrum. Third, following the design of vacuum ports in PEP-II [**heifets95**], the holes were drilled in rows. Slots were milled on the beam side of the holes that shielded the beam fields from seeing the transitions of each hole edge.

Potential Trapped Modes

We also used analytical estimates to ensure that our septum did not trap any EM modes that could create inter-bunch instabilities. We maintained the cross-sections to have approximately the same cutoff frequencies for both the dominant TE and TM modes as does the rest of the chamber. Numerical simulations done after the preliminary analytical designs verified the absence of trapped modes in the chamber.

DOWNSTREAM TRANSITION

As discussed above, most concerns on the impedance effects of the new septum chamber can be addressed through analytical analysis. However, due to the complex design of the downstream transition, we have to conduct numerical simulations to evaluate its impedance effects. The downstream transition serves as the connection between the septum chamber and the regular storage ring chamber. As shown in Fig. 3, it also combines the injected beam and stored beam chambers through an opening shaped like a beak. There are two effects of concern resulting from the "beak": the local heating due to the longitudinal wakefield and the beam instabilities caused by trapped RF modes. The latter can be avoided by careful mechanical design to prevent the formation of a low frequency resonant structure between the beam chamber and the surrounding bellows. In this section, we will present our efforts in evaluating the longitudinal wakefield by numerically calculating the longitudinal loss factor, k_l.

Numerical simulations have been carried out using a time-domain parallel code, T3P, running on the super computer, Cori, at the National Energy Research Scientific Computing Center (NERSC) [**NERSC**]. The simulation model mesh was constructed using CUBIT [**CUIBIT**]; the data was visualized using ParaView [**ParaView**].

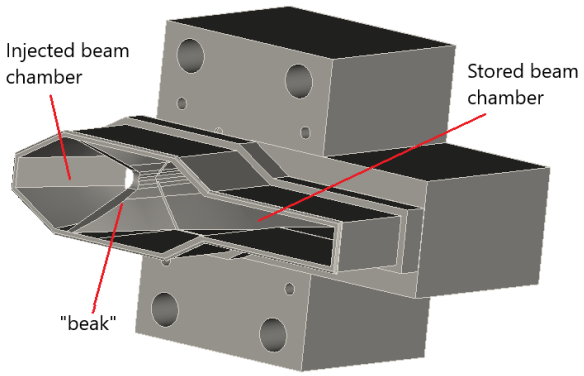

Figure 3: CAD model of the downstream transition.

Numerical Model

The impedance calculation of T3P applies an indirect integration method [**Nap93**], only suitable for cavity like structures, where the entrance and exit beam pipes intrude closer to the beam than any other part of the structure. The downstream transition chamber, of course, is not a cavity like structure. As a result, after building the model of the downstream transition chamber, we also need to intentionally create long transitions at both ends in order to minimize any calculational artifacts due to the end points of the calculation. The entire simulation model is shown in Fig. 4, where the highlighted part is the downstream transition with long tapers and short beam pipes added to both sides. To build the model of the downstream transition, we first individually create the injected beam chamber, the stored beam chamber, and the "beak", by lofting volumes through cross sections. Then we combine them together. As the chamber is created based on cross sections, it is straightforward to create a smaller cross section for the entrance and exit pipes. In the simulation, the rms bunch length of the beam is 6 mm with a Gaussian distribution. We choose the length of the entrance and exit beam pipes to be 10 times the rms bunch length of the beam, i.e. L1 = 60 mm in Fig. 4. The length of the tapered parts, L2, needs to be sufficiently long so that the additional impedance effects it contributes are negligible. Because the model has no rotational symmetry, the taper ratio varies azimuthally. However, for a value of L2 > 200 mm, the taper ratio is guaranteed to be larger than 10 in any direction. One should note that, due to the symmetry, only half of the structure is used for simulations. The symmetric plane is assigned to be a magnetic boundary and absorbing boundaries are assigned for all other open ports.

Simulation Results

First convergence tests on the sizes of the time steps and mesh were carried out. We found that the calculation results for the longitudinal wakefield showed little difference between time steps of $dt = 1$ ps and $dt = 0.8$ ps, therefore we picked $dt = 1$ ps. As shown in Fig. 5(a), the longitudinal wakefield was calculated and compared for different mesh sizes with our fixed time step of $dt = 1$ ps. The results changed significantly when the mesh size was reduced from 4 mm (blue) to 2 mm (red), but remained nearly identical when changing the mesh size from 2 mm to 1.5 mm (black). This suggests that 2 mm is a good choice for our mesh size. Similarly, in Fig. 5(b), we compared the results corresponding to different taper lengths, L2, and chose L2 = 300 mm.

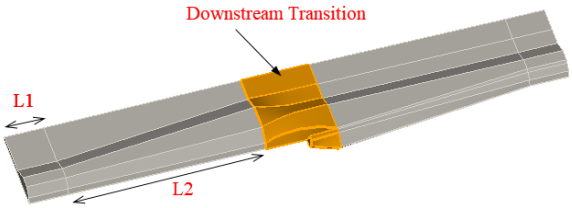

Figure 4: Numerical model of the downstream transition.

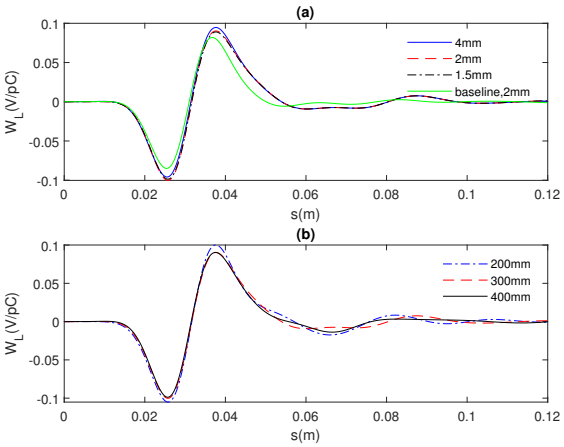

Figure 5: Longitudinal wake potentials calculated from T3P: (a) Runs for various mesh sizes; (b) Runs for various taper lengths, L2.

In order to calculate the extra impedance contribution for the "beak", we also created a baseline model by replacing the downstream transition with a smooth transition. The simulation results for this baseline model is shown by the green solid line in Fig. 5(a).

Based on the chosen numerical parameters, we calculate the longitudinal loss factor of transition chamber with the "beak" to be $k_l^{DT} = 0.0168$ V/pC, and that of the baseline model without the "beak" is $k_l^0 = 0.0082$ V/pC. Therefore the loss factor of the "beak" is $k_l^{\text{beak}} = 0.0086$ V/pC. The total longitudinal loss factor of SPEAR3 is roughly 10 V/pC, therefore the contribution from the downstream transition chambers for the new septum is a small fraction and negligible. The local heating can be calculated by using the longitudinal loss factor in the following equation:

$$P_l = k_l \cdot q \cdot I \tag{1}$$

where where P_l is the power loss from the beam, k_l is the longitudinal loss factor, q is charge per bunch, and I is the total stored beam current.For normal operation, SPEAR3 is filled with 500 mA in 280 bunches, therefore, from Eq.(1), we can calculate the local power contribution from the entire structure of the downstream transition to be about 11.7 W, and the contribution from the "beak" to be about 5.7 W.

CONCLUSION

The impedance effects of a new septum chamber have been studied both analytically and numerically. The results show that there are no major problems in either beam stability or local heating.

ACKNOWLEDGEMENTS

We want to thank C. Ng, L. Xiao, and Z. Li for their help and advice in the simulation studies, and B. Evanson for assistance in the CAD models.